

Spectral Mapping Tools from the Earth Sciences Applied to Spectral Microscopy Data

A. Thomas Harris*

Global Services Consultant, ITT Visual Information Solutions, Boulder, Colorado

Received 30 August 2005; Revision Received 16 March 2006; Accepted 14 April 2006

Background: Spectral imaging, originating from the field of earth remote sensing, is a powerful tool that is being increasingly used in a wide variety of applications for material identification. Several workers have used techniques like linear spectral unmixing (LSU) to discriminate materials in images derived from spectral microscopy. However, many spectral analysis algorithms rely on assumptions that are often violated in microscopy applications. This study explores algorithms originally developed as improvements on early earth imaging techniques that can be easily translated for use with spectral microscopy.

Methods: To best demonstrate the application of earth remote sensing spectral analysis tools to spectral microscopy data, earth imaging software was used to analyze data acquired with a Leica confocal microscope with mechanical spectral scanning. For this study, spectral training signatures (often referred to as endmembers) were selected with the ENVI (ITT Visual Information Solutions, Boulder, CO) “spectral hourglass” processing flow, a series of tools that use the spectrally over-determined nature of hyperspectral data to find the most spectrally pure (or spectrally unique) pixels within the data set. This set of

endmember signatures was then used in the full range of mapping algorithms available in ENVI to determine locations, and in some cases subpixel abundances of endmembers.

Results: Mapping and abundance images showed a broad agreement between the spectral analysis algorithms, supported through visual assessment of output classification images and through statistical analysis of the distribution of pixels within each endmember class.

Conclusions: The powerful spectral analysis algorithms available in COTS software, the result of decades of research in earth imaging, are easily translated to new sources of spectral data. Although the scale between earth imagery and spectral microscopy is radically different, the problem is the same: mapping material locations and abundances based on unique spectral signatures. © 2006 International Society for Analytical Cytology

Key terms: spectral microscopy; multispectral; hyperspectral; remote sensing; ENVI; confocal microscopy; spectral analysis; spectroscopy

Spectroscopy is the study of how materials uniquely absorb and emit light at different wavelengths based on their molecular composition. The technique has been used at a diverse range of scales, from studying the chemical makeup of stars, to investigating the molecular composition of a material under a microscope. Imaging spectroscopy, used for decades in the earth sciences for studying the earth's surface, is a technique for obtaining an image where each pixel (picture element) contains the complete spectral signature of the material within that pixel across a range of sampled wavelengths.

Earth imaging has its roots in aerial photography: shortly after the development of the camera in the mid-nineteenth century, French balloonists took the first photos of the ground from an aerial platform. Through both World Wars, aircraft photography was essential for reconnaissance and intelligence gathering, and then found utility in resource management and cartography. The first

aerial photographs were black and white, and then advanced to color. With the advent of infrared photography, the earth could be imaged at wavelengths that the human eye cannot detect. With the launch of the first earth-orbiting satellite, the Soviet Sputnik 1 in 1957, it wasn't long before the first images of the earth were captured from space by the American TIROS-1 weather satellite in April, 1960. Multispectral earth imaging, or imaging of the same area at a limited number of wavelengths of the electromagnetic spectrum, began in earnest in the early 1970s with the launch of the Landsat series of earth

*Correspondence to: A. Thomas Harris, ITT Visual Information Solutions, 4990 Pearl Circle East, Boulder, CO 80301, USA.

E-mail: tharris@itvis.com

Published online in Wiley InterScience (www.interscience.wiley.com).

DOI: 10.1002/cyto.a.20309

imaging satellites. The Landsat satellites, in operation through the present day, resulted in an unparalleled archive of the earth's surface and stimulated the development of a wide variety of methods for analyzing multispectral data.

Electromagnetic spectroscopy (herein referred to simply as spectroscopy) is the study of spectral signatures caused by the unique ways that materials interact with electromagnetic radiation. Many regions of the electromagnetic spectrum can be studied with spectroscopy, but in the context of earth imaging, the most important are the visible, infrared, and microwave, due to wavelength-specific atmospheric opacity. Imaging spectroscopy, often referred to as hyperspectral imaging, allows the collection of spectral signatures over some spatial area where each pixel contains the composite, mixed spectral signature of the materials contained within the pixel (1,2). A true hyperspectral instrument has many coregistered contiguous channels that sample very narrow portions of the electromagnetic spectrum, typically 10 nm or less. This "stack" of coregistered images is often referred to and visualized as an image cube (Fig. 1).

In the field of microscopy, spectral information can be collected through the use of either a wide-field or laser-scanning microscope. Although the methods for collecting spectral signatures differ with each approach, the result is the same: a stack of coregistered images where each x - y plane represents light detected from one small portion of the electromagnetic spectrum. Therefore, for the purposes of this study, different spectral data collection techniques will be referred to collectively as spectral microscopy. Note that this study is defining spectral microscopy data cubes as derived from a single x - y image plane; three-dimensional confocal imaging capabilities are not explored.

Recent advances in the field of spectral microscopy have in many ways mirrored those that took place in the last two decades in earth imaging. Early remote sensing studies were limited by multispectral imaging systems, characterized by few channels sampling radiation across relatively broad swaths of the electromagnetic spectrum. These systems could not differentiate subtle differences between materials because many objects on the earth's surface have similar signatures when measured channels are broad. Later, with the advent of hyperspectral imaging systems with considerably improved spectral resolution, earth scientists could discriminate materials with subtle differences in their spectral signatures, and for the first time, quantify their abundances. Similarly, conventional "multispectral" microscopy collected with band pass filters resulted in images that sampled broad portions of the electromagnetic spectrum, making it difficult to discriminate materials with strong signals in similar regions of the spectrum (3,4). However, with the advent of spectral imaging detectors for microscopes, and recent improvements in instrument calibration (5-7), it has become possible to discriminate spectrally similar materials based on their signatures across many channels. Although there are technical differences in data collection methods between spec-

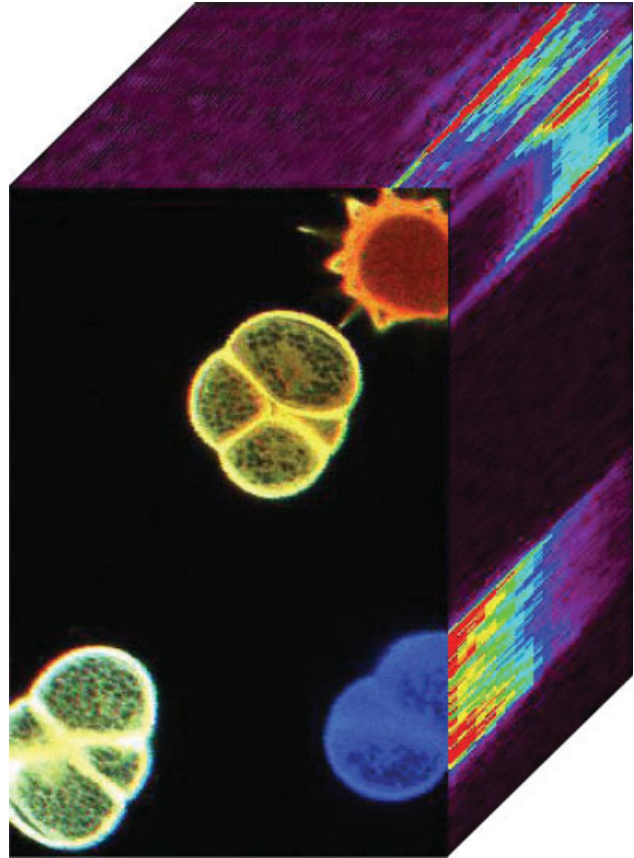


FIG. 1. An illustration of the pollen spore hypercube used in this analysis. The image on the "face" of the cube is an RGB color composite where Red = Band 10, Green = Band 5, and Blue = Band 1, and illustrates that each spore can be discriminated solely based on 3-band RGB color. The sides of the "image cube" show the relative intensities of edge pixel values across the spectral dimension in 20 bands from 600-700 nm in the visible orange and red wavelengths of the electromagnetic spectrum.

tral microscopy and hyperspectral remote sensing, the end product is similar: a signal measured in many channels across the visible and near infrared portions of the electromagnetic spectrum. Therefore, many of the analysis methods developed for earth imaging applications can be directly applied to spectral microscopy data cubes.

Several studies have used analysis techniques originally developed in the earth sciences for spectral microscopy analysis. The most widely used methods include both supervised classification techniques (8,9) and linear spectral unmixing (LSU) (3,4,8-11). All of these studies demonstrated success utilizing these techniques with spectral microscopy data. On the basis of the success of these previous studies, it stands that other spectral analysis techniques developed for use with earth imaging and imaging spectrometer data would translate for use with spectral microscopy data cubes.

Many of the techniques developed for application with earth imaging data were created to improve on limitations of previously used methods. For example, LSU is based on the assumption that pixel signatures are linear combina-

tions of known material signatures that exist within the image, often referred to as endmembers. This assumption is often violated, such as when pixel signatures are the result of nonlinear multiple scattering (5) or in cases where the signatures from two or more materials are mixed at the molecular level, such as in two combined liquids (1). In addition, if all the spectrally distinct materials in an image are not adequately defined, or if intensities of spectral training signatures do not match the intensities of image spectra, errors in modeling the composition of each image pixel can be large. These limitations led to the development of other, more robust techniques for material mapping. For example, the matched filter, a technique originally developed for use in signal processing, allows an analysis to proceed based on a search for an individual signature, without having to define all spectrally distinct materials in a hyperspectral data cube. The matched filter is just one of many algorithms that have been developed to work with imaging spectrometer data, all of which are directly applicable to image data cubes acquired through spectral microscopy. The goal of this analysis is to demonstrate a cross-section of the varied approaches originally developed in the field of earth remote sensing that are available and easily translated for use with spectral microscopy data cubes.

MATERIALS AND METHODS

Data Acquisition

As an illustration of how techniques developed for application in the earth sciences can be easily translated to spectral microscopy, a 20-band image in the wavelength range between 600 and 700 nm was acquired of a sample slide containing three types of pollen spores (Carolina Biological Supply Company, Burlington, NC) using a Leica TCS-SP1 confocal spectral imaging system with mechanical spectral scanning (Fig. 1). The pollen spore slide was excited with a 568 nm laser and fluorescent emission was measured at a 5 nm band-pass. Individual image bands were loaded into ENVI using a custom data ingestion program written in IDL (ITT Visual Information Solutions, Boulder, CO).

Data Preprocessing

Zimmerman et al. (4) point out some of the challenges of spectral microscopy such as background mixing and low signal-to-noise ratio. There was considerable band-to-band noise in this data set. Therefore, ENVI was used to calculate a two-band average to increase the signal-to-noise ratio of the data set, and resulted in 10 output bands. Next, an image mask was developed that was applied to remove both saturated pixels (those pixels with any channel having the maximum digital number value of 256) and those pixels related to the slide background, or those areas in the image where there were no pollen spores. This was done so that only unsaturated pixels that contained pollen spores would remain for analysis.

Typical ENVI Spectral Analysis Work Flow

Analyzing spectral microscopy data is identical in many ways to analyzing data collected by an imaging spectrometer. The major difference is one of scale: an image acquired by an imaging spectrometer encompasses square kilometers, while an image acquired through spectral microscopy may be square microns in size. Regardless, the problem remains to identify different materials in the image based on their spectral signatures. In most image analysis scenarios utilizing ENVI, this problem is typically broken down into two steps (Fig. 2). First, training signatures are developed. Training signatures, often referred to as spectral endmembers, are good examples of the different "pure" materials that can be found in the image. Second, every pixel in the image is compared to the endmembers to measure similarity. This step can be carried out using a variety of the available algorithms within ENVI, from general purpose supervised classification, to specialized hyperspectral analysis tools.

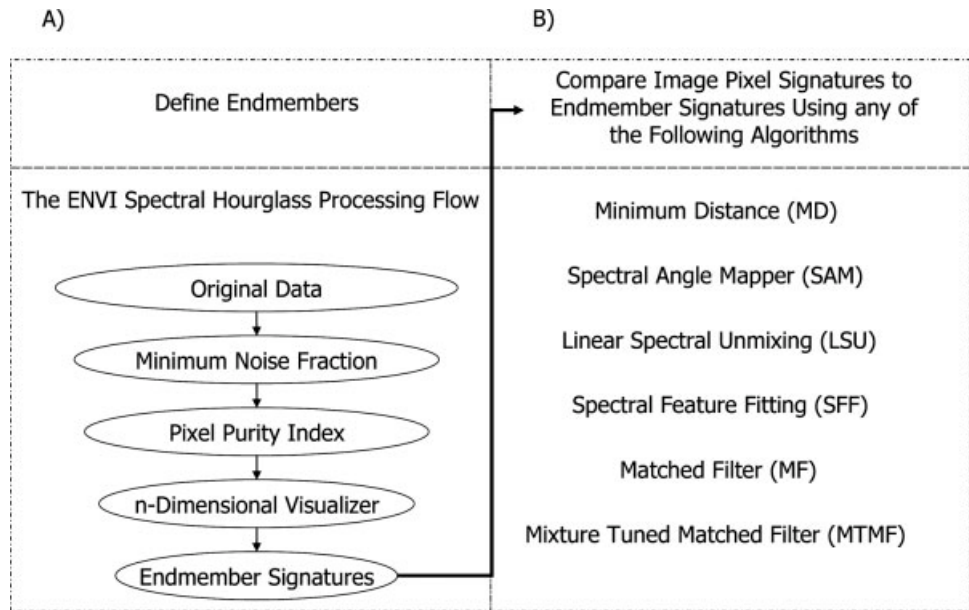
Defining Endmembers

The first step in any analysis is to define endmembers, or training signatures, to map in the data cube (Fig. 2). Two approaches are available: (1) in-scene--identifying pixels in the image that are good representations of the materials to be mapped, or (2) external source--using signatures from some other source, such as from another material sample (i.e., in a spectral library). Both methods are fully supported in ENVI and provide the required data for subsequent analysis. However, when available, in-scene endmembers have several advantages. For example, most spectral microscopy systems allow the gain to be adjusted on instrument photo multiplier tubes (PMT); if external-source spectral endmember signatures are recorded at a different time than the image to be analyzed, precautions must be taken to ensure that gain factors match (3). Additionally, changes in pH and ion concentrations can have marked effects on the spectral response of a sample, necessitating caution when using external-source spectral endmembers. For these reasons, it can be advantageous to extract endmember signatures directly from the image to be analyzed. This is the approach followed in this study.

Finding Image Endmembers

Many software utilities available to the spectral microscopist for pixel unmixing have limited capabilities for selecting pixels for use as spectral endmembers. For example, the Zeiss LSM 510 META laser scanning microscope includes spectral unmixing software but is limited because the analyst must select pixels to use as endmembers "by hand." For this analysis, pixels within the spore data cube were chosen as representative endmembers using three algorithms that together comprise the ENVI Spectral Hourglass™ processing flow: the minimum noise fraction rotation (MNF), the pixel purity index (PPI), and the *n*-Dimensional Visualizer™ (Fig. 2A). The hourglass processing flow used the spectrally over-determined nature of hyperspectral data to find the most spectrally pure

FIG. 2. The ENVI processing workflow. Any supervised image classification can be subdivided into two steps: (A) Definition of endmember signatures, and (B) measurement of similarity between unknown pixel signatures and each endmember signature. The ENVI Spectral Hourglass™ processing flow (A) was used to spatially and spectrally subset the data set and to find the most spectrally pure (or spectrally unique) pixels (called endmembers). These endmember signatures were then using in a range of mapping algorithms, listed in (B).



(or spectrally unique) pixels (endmembers) within a data cube, and is, therefore, a more robust method than simply selecting pixels for use as endmembers “by hand.” This method is referred to as the “Spectral Hourglass,” because with each step of the processing flow, data is removed from the analysis, increasing the efficiency of processing.

The first step in the hourglass processing flow was the MNF rotation, a process that determined the inherent dimensionality (i.e., number of possible endmembers) of the spore data set, segregated noise in the data, and reduced the computational requirements for subsequent processing (12). The MNF transform, as implemented in ENVI, is modified from Green et al. (13) and is essentially a double, or cascaded principal components transformation that results in a data space that can be divided into two parts: one part associated with coherent signal, and a complementary part dominated by noise. By using only the coherent portions in subsequent processing, the noise was separated from the data, reducing the size of the data set, and improving results. MNF results also indicated the true dimensionality of the dataset: the number of MNF bands containing coherent signal is approximately equal to the number of unique endmembers in the dataset.

The Pixel Purity Index™ (PPI) was used to find the most spectrally pure (extreme or unique) pixels in the image data cube. In general, the most spectrally pure or unique pixels typically correspond to mixing endmembers. The PPI was computed by repeatedly projecting n -dimensional scatterplots onto a random unit vector. The extreme pixels in each projection (those pixels that fell onto the ends of the unit vector) were recorded and the total number of times each pixel was marked as extreme was noted. A pixel purity image was created in which the DN of each pixel corresponded to the number of times that pixel was recorded as extreme (14). The pixel purity

image was then analyzed to find those pixels that were most frequently found in extreme positions during the random projections (i.e., the most spectrally unique pixels). The pixel purity image resulted in a total of 44 pixels being identified as spectrally unique. However, this set represented a heterogeneous mixture of signatures. In order to cluster together these pixels into individual endmembers, they were input into the final step of the spectral hourglass processing flow, the n -Dimensional Visualizer.

The n -Dimensional Visualizer was used to interactively locate, identify, and cluster the most spectrally pure or unique pixels in the image cube by visualizing those pixels selected from the PPI as points in an multidimensional scatterplot, where the number of dimensions was defined by the total number of coherent MNF bands (15). The advantage of the n -Dimensional Visualizer was that it allowed visualization of points in an n -dimensional space, forming a data “cloud.” The number of endmembers and their signatures were estimated by selecting pixel points at the corners of the data cloud. A total of 10 individual pixels divided among four distinct endmembers were selected from the n -Dimensional Visualizer. Final endmember signatures were calculated by finding the average signature from all pixels in each group, and are depicted in Figure 3.

Image Classification

Once endmember signatures are defined, the next step in an analysis workflow is to compare every pixel in the image to the endmember signatures and measure similarity using a classification or spectral mapping algorithm. There are many classification algorithms to choose from in ENVI, ranging from those designed primarily for use with

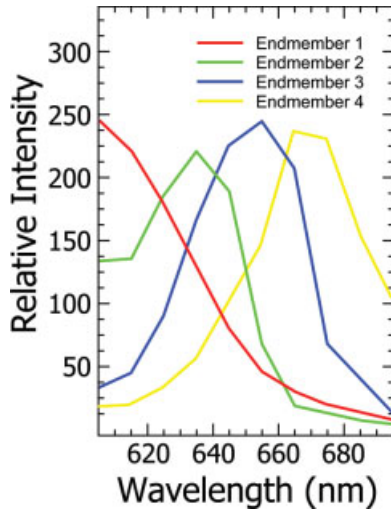


FIG. 3. Endmember spectra from the ENVI Spectral Hourglass™ processing flow used in six mapping algorithms.

multispectral imagery, to those designed specifically for use with hyperspectral data sets. Each algorithm is distinct, all taking different approaches to comparing image spectral signatures to endmember signatures. For example, the spectral angle mapper (SAM) (Fig. 4, top panel) is an algorithm that evaluates similarity between image and endmember spectra by treating them as vectors in an n -dimensional space where the number of dimensions is equal to the number of bands, and measuring the angle between vectors. Smaller angles represent closer matches to the reference spectrum. In marked contrast, the spectral feature fitting (SFF) algorithm (Fig. 4, bottom panel) measures similarity by evaluating the physical shape of spectral signatures. For each unknown image spectrum, scale, or the measure of absorption feature depth relative to the endmember spectrum is calculated. In addition, the unknown image and endmember spectra are compared at each selected wavelength in a least-squares sense and the root mean square (RMS) error is determined for each image spectrum. Those pixels with high scale and low RMS are deemed close matches.

For this study, six separate mapping algorithms were applied to the image data cube: the minimum distance classifier (MDC), the spectral angle mapper (SAM), linear spectral unmixing (LSU), spectral feature fitting (SFF), the matched filter (MF), and the mixture tuned matched filter (MTMF). The MDC computes a single metric for each pixel, the Euclidean distance from each unknown pixel to the mean of each endmember. This algorithm was originally designed for use with multispectral data, but had utility in this application because of the limited numbers of bands and endmember signatures. Similarly, the SAM algorithm resulted in a single measure of each pixel spectral angle from the mean of each endmember signature (Fig. 4, top panel). As mentioned previously, and illustrated in Figure 4 (bottom panel), the SFF algorithm resulted in two parameters for each endmember: (1) a scale image that

measured the depth of each pixel's absorption feature relative to the endmember signature, and (2) an RMS image that measured the band-to-band "goodness of fit" of each pixel signature to the endmember signature. Close matches for each endmember were those pixels with a high scale and low RMS. Therefore, dividing the scale by the RMS image created a single output image for each endmember where close matches were the pixels with the highest values. LSU models each spectrum as a linear combination of known endmembers, and resulted in a sub-pixel fractional abundance measure for each endmember. As mentioned previously, LSU results are very sensitive to the set of endmember signatures used, necessitating careful definition of all endmember signatures in the image. In contrast, both the MF and MTMF methods provide partial unmixing based on individual endmember signatures by maximizing the difference between the chosen endmember and the unknown background. These methods tend to be more robust and also result in subpixel abundances for each endmember. The MTMF uses the same algorithm as MF but additionally computes a measure of feasibility, which can be used to reduce false positives, a problem common to MF.

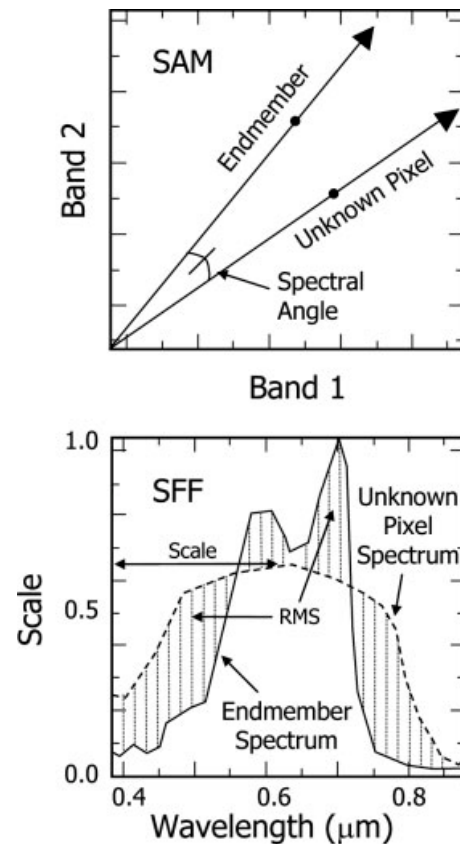
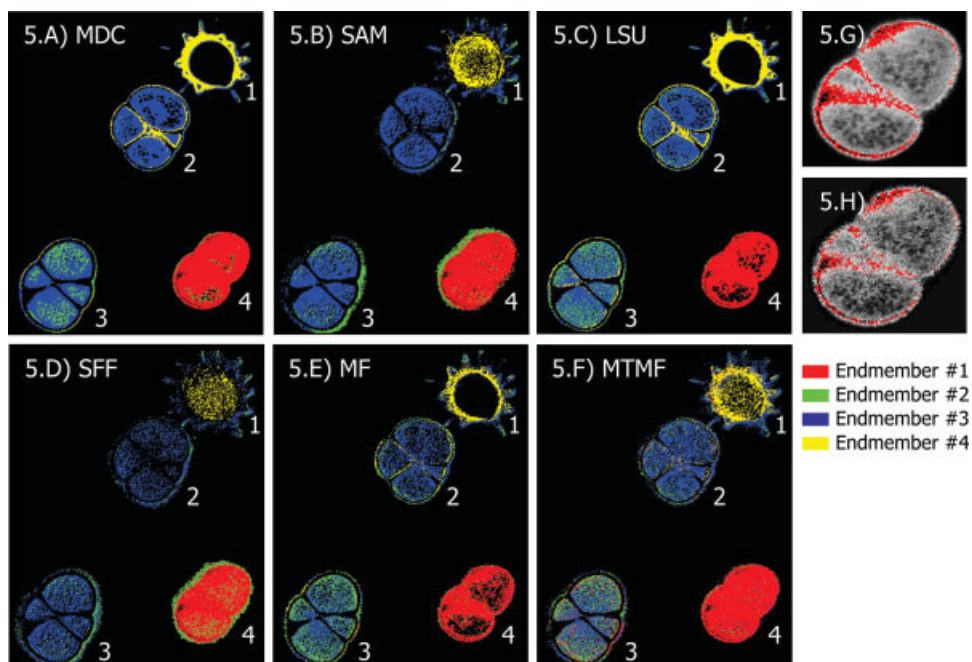


FIG. 4. An illustration of the difference in the way that two spectral mapping algorithms, the spectral angle mapper (SAM, top panel) and spectral feature fitting (SFF, bottom panel), approach the problem of comparing a known endmember signature to an unknown pixel signature.

FIG. 5. Results of an analysis using endmember signatures derived from the ENVI Spectral Hourglass™ processing flow. Classification images for six separate algorithms are shown: (A) the minimum distance classifier (MDC), (B) the spectral angle mapper (SAM), (C) linear spectral unmixing (LSU), (D) spectral feature fitting (SFF), (E) the matched filter (MF), and (F) the mixture tuned matched filter (MTMF). With rich spectral information, it is possible to resolve subpixel fractions of materials. G–H shows gray-scale images of Endmember 1 from the LSU and MF methods respectively. Endmember 1 occurs primarily within Spore 4 in the classification images. Pixels highlighted in red are those that contain at least 80% of Endmember 1.



Any time an algorithm is used with spectral endmembers to map materials in an image, each pixel will have a value representing that pixel's similarity to each endmember signature. It is the analyst's responsibility to choose the value that represents the cutoff for each class. This technique is referred to as defining the threshold for each class, and is central to the idea of supervised classification. For example, the SAM algorithm measures the n -dimensional spectral angle of every pixel in an image to every endmember signature. For every endmember, the analyst must determine the maximum spectral angle, beyond which pixels are excluded from the respective class. For each mapping method, a threshold value was visually determined for each endmember rule image, resulting in a final classification image. Reflecting the "supervised" nature of spectral classification, threshold values were chosen based on that value for each endmember that resulted in a similar material map across the six mapping methods. Single band classification images were then generated based on the selected threshold values, where endmember signatures were mapped in the image by assigning individual pixels to classes. Finally, to illustrate the subpixel concentration mapping capabilities of the two algorithms LSU and MF, a threshold of 0.80 was applied to the Endmember 1 concentration image resulting in regions of interest (ROIs) for all those pixels containing at least 80% Endmember 1.

RESULTS

For reference, an RGB color composite image is displayed in Figure 1, where the red, green, and blue color channels contain bands 10 (695 nm), 5 (645 nm), and 1 (605 nm), respectively. Note the color differences between the various pollen grains, indicating that materials

in the image are spectrally distinct based on the three displayed bands.

Figures 5A–5F show the final results from the six mapping algorithms: the MDC (Fig. 5A), the SAM (Fig. 5B), LSU (Fig. 5C), SFF (Fig. 5D), the MF (Fig. 5E), and the MTMF (Fig. 5F). The six classification results are similar, but not identical, reflecting differences in the mechanics of the six classification algorithms; all techniques approach the problem of spectral classification in different ways. Note that, in general, each of the algorithms did an acceptable job of discriminating the three spore types. In all cases, Endmember 3 is mapped at the periphery of Spore 1, indicating that the intensity spectra from those pixels are similar to Endmember 3. There are several differences between the classification methods, the most obvious being those pixels that are mapped as belonging to Class 4 (Yellow). The MDC (Fig. 5A), LSU (Fig. 5C), and MF (Fig. 5E) algorithms found that those pixels at the periphery of Spore 1 belonged to Class 4 (Yellow), while the SAM (Fig. 5B), SFF (Fig. 5D), and MTMF (Fig. 5F) mapped pixels from the periphery and interior of Spore 1 into Class 4. Also, Endmember 2 is mapped at the periphery of Spores 2 and 3 in some, but not all, of the algorithms. A final obvious difference between the six methods relates to the spatial coherence of the results. For example, the MDC (Fig. 5A) has the highest degree of spatial coherence, with pixels in various classes clustered together in well-defined groups. Alternatively, the SFF algorithm resulted in relatively low spatial coherence, understandable given that the SFF algorithm is ideally used for finding pixels with specific absorption features in their signatures (Fig. 4, bottom panel); in this application, the fluorescent emission signatures did not contain specific, molecular-based absorptions. Note, however, that SFF could find utility in spectral fluorescence applications where molecular absorption is an important process.

Table 1
Number of Pixels Classified as Each Endmember and Percentage of Total for Each of the Six Classification Methods

Endmember	MDC		SAM		LSU		SFF		MF		MTMF	
	No. of points	% Total	No. of points	% Total	No. of points	% Total	No. of points	% Total	No. of points	% Total	No. of points	% Total
Unclassified	94,895	83.2	95,117	83.4	95,455	83.8	98,829	86.7	99,456	87.2	94,258	82.7
Endmember 1 [Red]	5,258	4.6	5,388	4.7	4,700	4.1	5,003	4.4	3,971	3.5	6,551	5.7
Endmember 2 [Green]	1,873	1.6	2,094	1.8	2,266	2.0	2,477	2.2	2,937	2.6	2,487	2.2
Endmember 3 [Blue]	9,641	8.5	9,320	8.2	8,591	7.5	6,601	5.8	6,147	5.4	8,414	7.4
Endmember 4 [Yellow]	2,333	2.1	2,081	1.9	2,988	2.6	1,090	1.0	1,489	1.3	2,290	2.0
<i>Total</i>	<i>114,000</i>	<i>100</i>	<i>114,000</i>	<i>100</i>	<i>114,000</i>	<i>100</i>	<i>114,000</i>	<i>100</i>	<i>114,000</i>	<i>100</i>	<i>114,000</i>	<i>100</i>

MDC, Minimum distance classifier; SAM, spectral angle mapper; LSU, linear spectral unmixing; SFF, spectral feature fitting; MF, matched filter; MTMF, mixture tuned matched filter.

The similarity of the mapping methods is illustrated statistically in Table 1 that shows both the number of pixels, and the percentage of total, for each class. Table 1 shows that all six mapping methods resulted in roughly the same percentage of pixels assigned to each class, and it illustrates the utility of any of the methods for mapping applications in spectral microscopy.

Similar to LSU, there are several algorithms that result in subpixel fractional abundance of endmember signatures, specifically the MF, MTMF, and SFF algorithms. All three provide a scale statistic that is related to subpixel fractional concentration of materials. Figures 5G–5H show gray-scale images of Endmember 1 subpixel concentration from the LSU and MF methods respectively for the area labeled as Spore 4 in the classification images. Both images had a threshold applied to highlight pixels that contain at least 80% of Endmember 1. The similarity of the MF and LSU results illustrates how the MF could find utility as a technique for quantification of subpixel fractions of materials. It is worth noting that the results are not identical: it is the analyst's responsibility to determine which method has the most utility for the task at hand.

DISCUSSION AND CONCLUSIONS

This study was conducted to demonstrate spectral analysis tools developed in the field of earth remote sensing, and to show how they can be translated for use with spectral microscopy data. Although the scale difference between earth remote sensing and spectral microscopy data is extreme, the basic characteristics of the data and the problems facing spectral microscopists and earth remote sensing scientists are the same. For example, a common problem in fluorescent microscopy is that a material of interest is not differentiated from the background when fluoresced at a particular wavelength. This is precisely the problem that earth-imaging scientists dealt with for decades and that was resolved through the use of multi- and hyperspectral imaging technology, allowing the discrimination of similar materials based on subtle differences in spectral signatures.

The results illustrated in Figure 5 and Table 1 show that, while each spectral mapping algorithm gave slightly differ-

ent results, results were spatially and statistically similar, suggesting that spectral identification algorithms other than the previously used supervised classification (8,9) and LSU (3,4,8–11) will have utility for spectral microscopy. Moreover, these results showed that a full range of algorithms could be used to derive similar results, providing the analyst with a host of options for solving any particular spectral analysis problem. It should be noted that this study included no analysis of which algorithm was most suitable for discriminating individual spore structures; lacking "truth" data made that analysis infeasible.

Use of the LSU technique in spectral microscopy has come out of the express desire to resolve subpixel fractional abundances of materials. This analysis introduced and demonstrated two techniques for resolving subpixel material concentrations: the MF and MTMF, both techniques that have yet to be widely used in the field of spectral microscopy. These techniques have the advantage of allowing an analyst to search for a single signature in a spectral data set, without having to define all image endmembers, a limitation of the LSU technique. Also, as pointed out previously, LSU assumes that pixel signatures are linear combinations of defined endmembers. In reality, pixel signatures recorded at the cellular level will likely be highly nonlinear because of interactions between endmembers occurring at the molecular level (1). Therefore, having alternative methods at the analyst's disposal can be critically important.

The goal of this investigation was to highlight techniques developed for spectral analysis in the earth sciences that have potential for contributing to the field of spectral microscopy. As illustrated in this investigation, there are a number of spectral analysis algorithms available to the spectral microscopist that have yet to be widely utilized, pointing at new and potentially rewarding avenues of research.

LITERATURE CITED

1. Clark RN. Spectroscopy of rocks and minerals, and principles of spectroscopy. In: Rencz AN, editor. *Manual of Remote Sensing*, Vol. 3: *Remote Sensing for the Earth Sciences*. New York: Wiley; 1999. pp 3–58.
2. Green RO, Eastwood ML, Sarture CM, Chrien TG, Aronsson M, Chippendale JA, Pavri BE, Chovit CJ, Solis M, Olah MR, Williams O.

- Imaging spectroscopy and the airborne visible/infrared imaging spectrometer (AVIRIS). *Rem Sens Environ* 1998;65:227-248.
3. Berg RH. Evaluation of spectral imaging for plant cell analysis. *J Microsc* 2004;214:174-181.
 4. Zimmermann T, Rietdorf J, Pepperkok R. Spectral imaging and its applications in live cell microscopy. *FEBS Lett* 2003;546:87-92.
 5. Lerner JM, Zucker RM. Calibration and validation of confocal spectral imaging systems. *Cytometry Part A* 2004;62A:8-34.
 6. Zucker RM, Chua M, Salmon W, Rigby P, Clements I. Reliability of confocal spectral imaging systems: Use of multispectral beads. *Cytometry A*. This issue.
 7. Zucker RM, Lerner JM. Wavelength and alignment tests for confocal imaging systems. *Microsc Res Tech* 2005;68:307-319.
 8. Kocanova S, Mateasik A, Chorvat D Jr, Miskovsky P. Multispectral confocal fluorescence imaging: Monitoring of intracellular distribution of PKC influenced by photoactive drug hypericin. *Laser Phys Lett* 2005; 2:43-47.
 9. Lansford R, Bearman G, Fraser SE. Resolution of multiple green fluorescent protein color variants and dyes using two-photon microscopy and imaging spectroscopy. *J Biomed Opt* 2001;6:311-318.
 10. Ecker RC, de Martin R, Steiner GE, Schmid JA. Application of spectral imaging microscopy in cytomics and fluorescence resonance energy transfer (FRET) analysis. *Cytometry Part A* 2004;59A:172-181.
 11. Dickinson ME, Bearman G, Tille S, Lansford R, Fraser SE. Multi-spectral imaging and linear unmixing add a whole new dimension to laser scanning fluorescence microscopy. *Biotechniques* 2001;31:1272-1278.
 12. Boardman JW, Kruse FA. Automated spectral analysis: A geological example using AVIRIS data, north Grapevine Mountains, Nevada. In: *Proceedings of the Tenth Thematic Conference on Geologic Remote Sensing*. Ann Arbor, MI: Environmental Research Institute of Michigan (ERIM); 1994. pp 1-407-1-418.
 13. Green AA, Berman M, Switzer P, Craig MD. A transformation for ordering multispectral data in terms of image quality with implications for noise removal. *IEEE Trans Geosci Rem Sens* 1988;26:65-74.
 14. Boardman JW, Kruse FA, Green RO. Mapping target signatures via partial unmixing of AVIRIS data. *Summaries of the Fifth JPL Airborne Earth Science Workshop* 1995;1:23-26. JPL Publication No. 95-1.
 15. Boardman JW. Automated spectral unmixing of AVIRIS data using convex geometry concepts. *Summaries of the Fourth JPL Airborne Geoscience Workshop* 1993;1:11-14. JPL Publication No. 93-26.